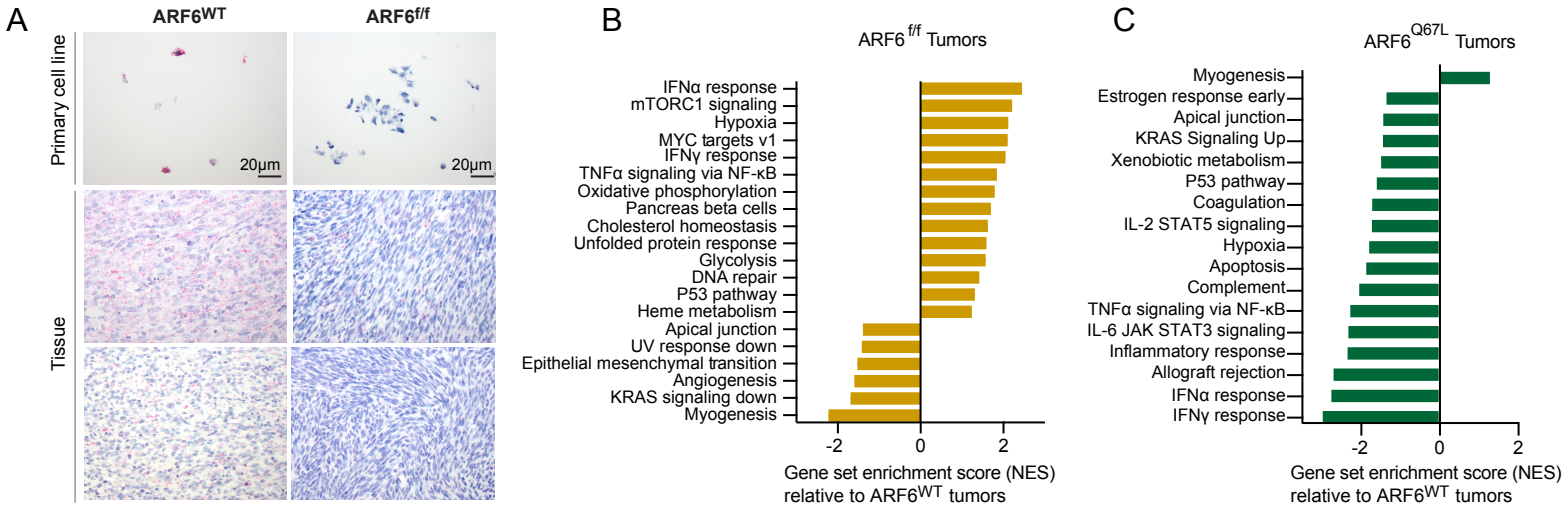

Figure S1: *Arf6* expression and ARF6-dependent gene expression pathways in murine tumors, related to Figures 1, 2.
(A) In situ hybridization detection of *Arf6* mRNA (pink). Left panels show expected diffuse signal. Right panels show expected loss of signal. Right middle panel shows representative low-level heterogenous *Arf6* signal in murine tumor 19835, consistent with the low level of ARF6 detected by Western blot for the 19835 primary tumor cell line (see Figure 1G). **(B and C)** Bulk tumor transcriptomes (RNAseq) with significantly enriched gene sets (MSigDB Hallmark) in $ARF6^{f/f}$ **(B)** and $ARF6^{Q67L}$ **(C)** tumors compared to $ARF6^{WT}$ control tumors.

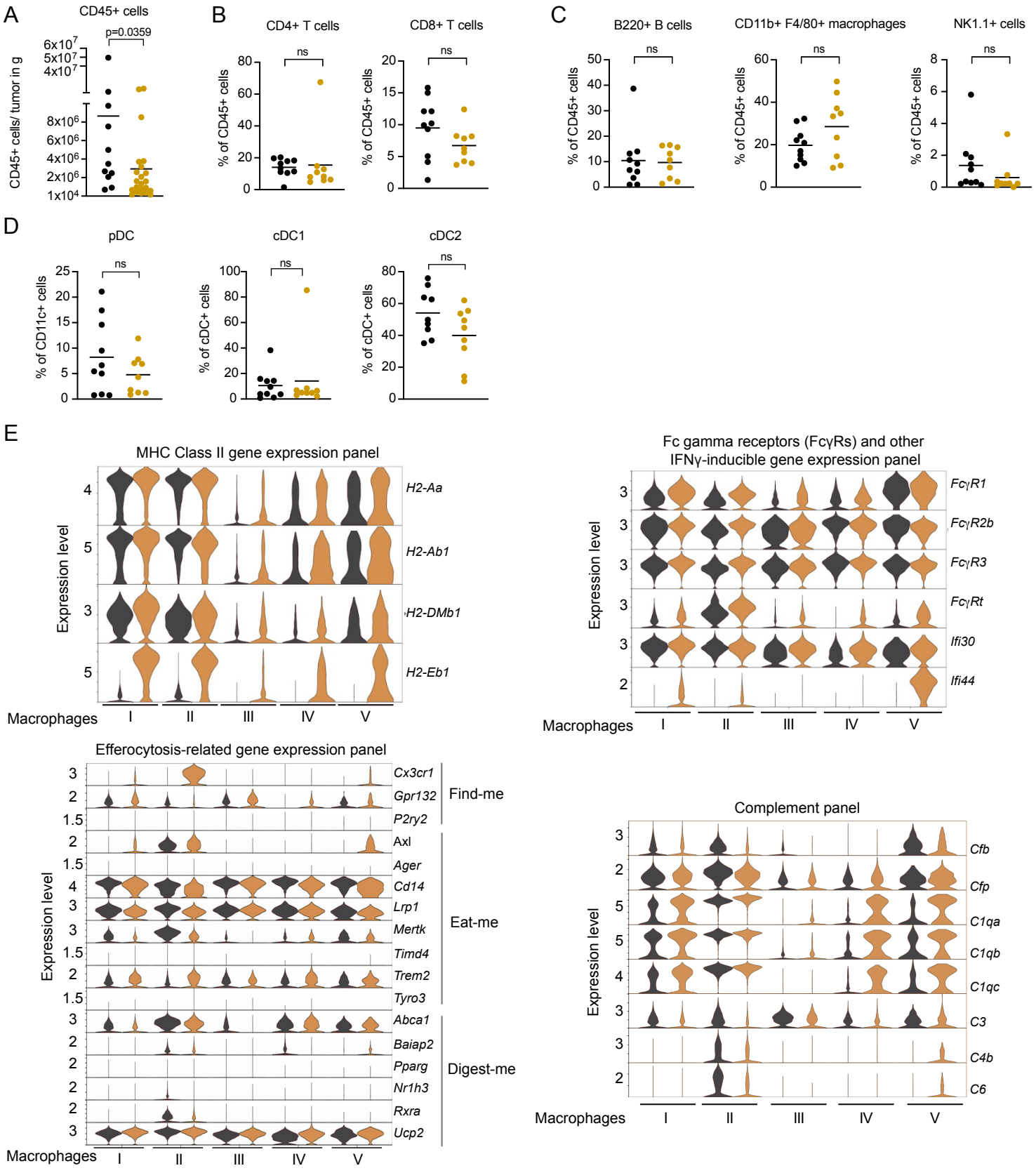

Figure S2: Immune profiling of tumor microenvironment, related to Figure 3.
(A) The absolute numbers of CD45$^+$cells per gram of tumor. **(B)** Fractions of CD4$^+$and CD8$^+$ T cells in CD45$^+$cells. **(C)** Fractions of B220$^+$B cells, CD11b$^+$F4/80$^+$ macrophages, and NK1.1$^+$cells in CD45$^+$cells. **(D)** Fractions of plasmacytoid dendritic cells (pDC) and conventional dendritic cell subsets (cDC1 and cDC2). **(A-D)** Graphs represent mean. Two-tailed Mann-Whitney t-test. **(E)** Expression of IFNγ-inducible genes related to antigen presentation (MHC Class II), phagocytosis (FcγR and other genes), efferocytosis-related genes and Complement genes, across different subtypes of macrophages. A comprehensive list of adjusted p-values, obtained from Seurat's Wilcoxon Rank Sum test for differentially expressed genes, is provided in Table S2.

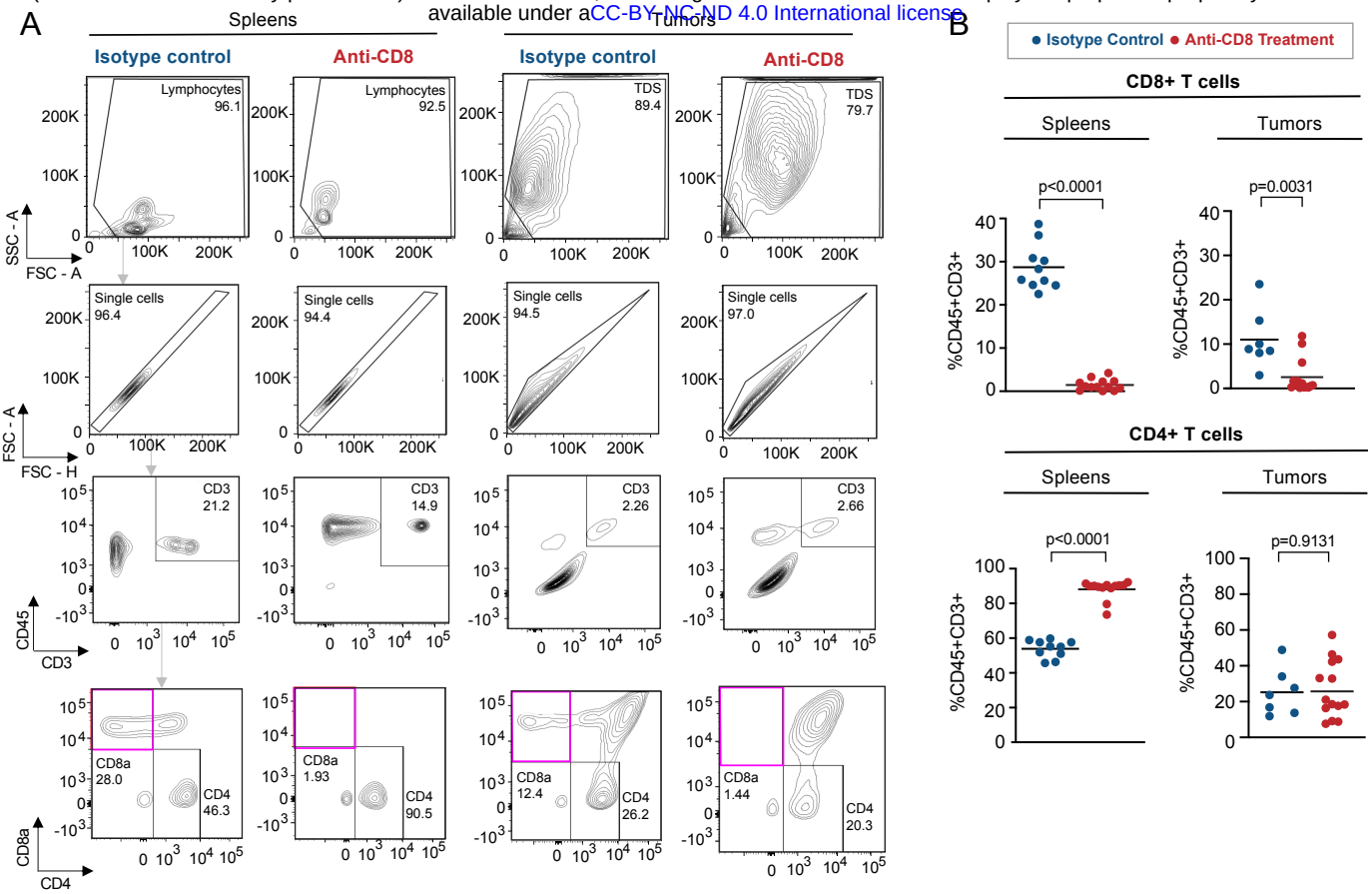

Figure S3: Efficiency of CD8 T cell depletion, related to Figure 3.
(A and B) Quantitation of T cells by flow cytometry **(A)** and graph representing the mean **(B)** in spleens and tumors of mice treated with isotype control (IgG2b) or anti-CD8 antibody. Two-tailed Mann-Whitney t-test.

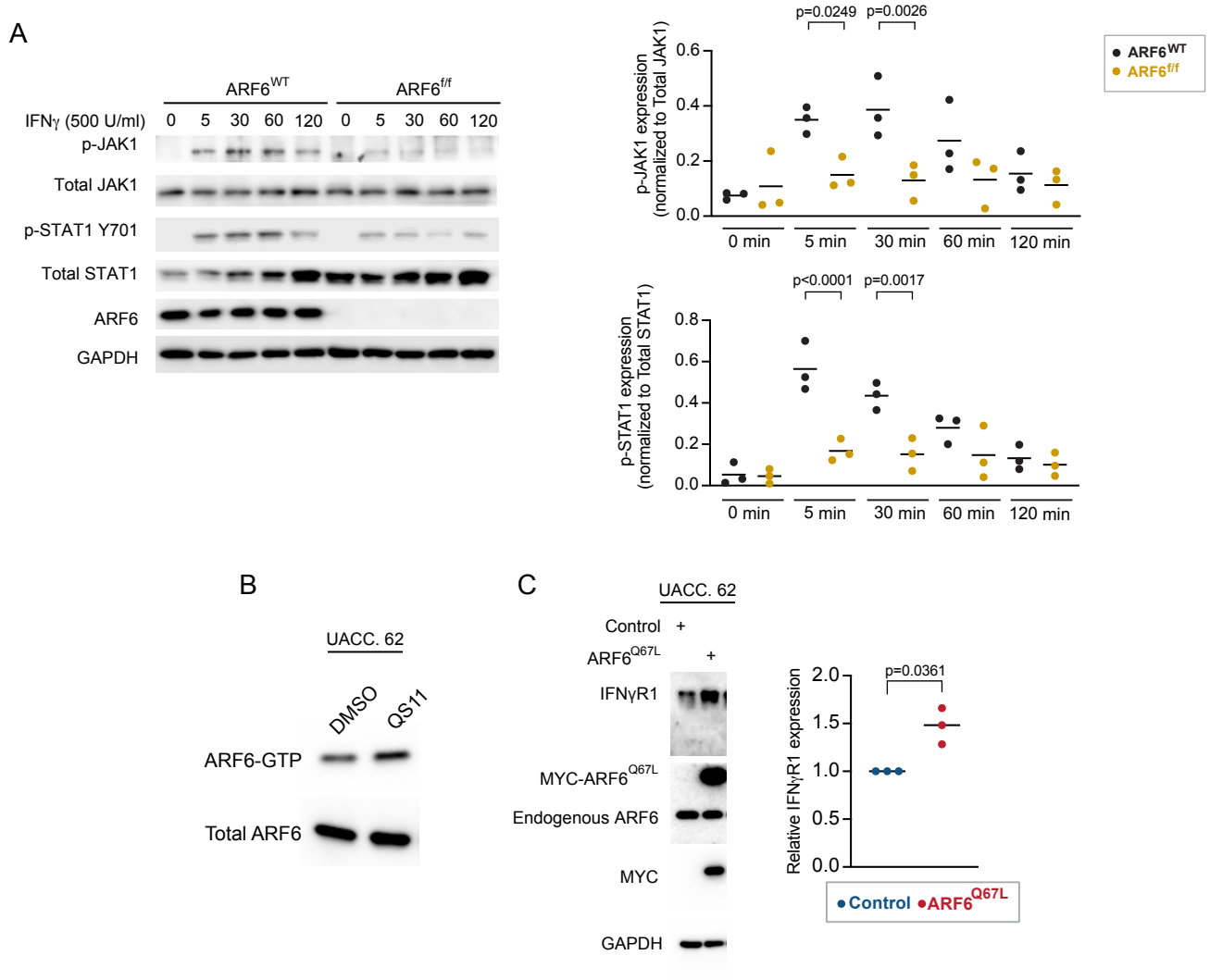

Figure S4: Tumor-intrinsic ARF6-dependent IFNγ signaling, related to Figure 4.
(A) IFNγ-induced JAK-STAT signaling detection in early-passage murine melanoma cell lines. n=3 replicates each. Two-way ANOVA with Tukey's multiple comparisons test. **(B)** Total ARF6 and ARF6 GTP pulldown in UACC.62 cells without or with 2μM QS11 treatment for 1hr. **(C)** Western blot for indicated proteins in UACC.62 cells without or with adenoviral-mediated ectopic expression of constitutively active ARF6 ($ARF6^{Q67L}$), control= empty vector, n=3 biological replicates. Ratio paired t-test.

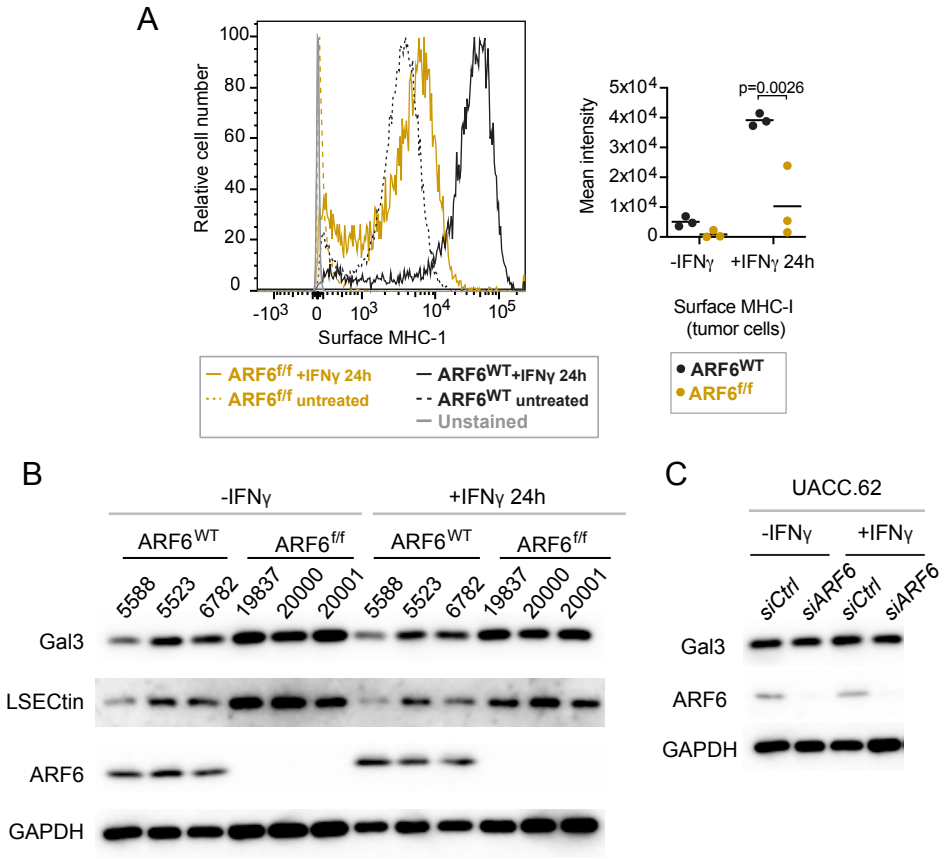

Figure S5: Expression of MHC-1 and LAG3 ligands, related to Figure 5.
(A) Flow cytometric detection of tumor cell surface MHC-I expression, n=3 independent cell lines of each genotype. Two-way ANOVA test. **(B)** Western blot detection of Galectin3 (Gal3) and LSECtin in murine melanoma, n=3 independent cell lines of each genotype. **(C)** Western blot detection of Gal3 in UACC.62 cells without or with ARF6 knockdown, n=3 biological replicates.

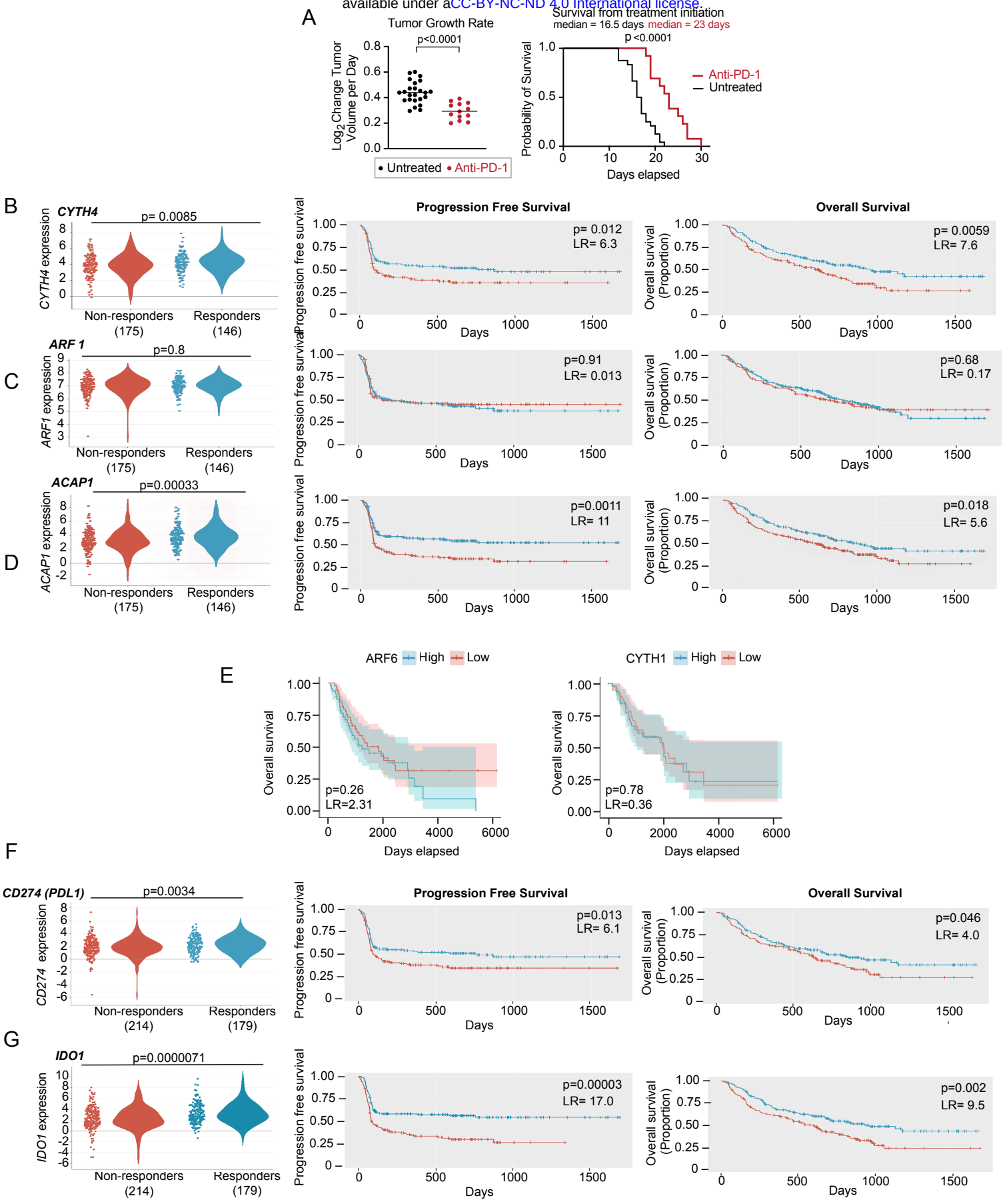

Figure S6: ICB treatment outcomes, related to Figure 6.
(A) Systemic anti-PD-1 treatment initiated in *Arf6*^{WT} mice with established tumors (up to 5mm in greatest dimension, 27-72mm^3). Untreated controls (n=24), anti-PD-1 (n=13). Rate of tumor growth measured from initiation of treatment, Welch's t-test. Survival (primary tumor reached 2cm) from initiation of treatment, Log-rank (Mantle-Cox) test. **(B-D)** Association of ICB treatment outcome in melanoma patients with mRNA levels of *CYTH4* **(B)**, *ARF1* **(C)** and *ACAP1* **(D)** in transcriptomes of pretreatment melanoma biopsies (CancerImmu expression analysis). **(E)** Lack of association of *ARF6* and *CYTH1* expression (tumor) with survival of non-ICB treated melanoma patients (TCGA, n=163). **(F-G)** Association of ICB treatment outcome in melanoma patients with mRNA levels of *CD274* **(F)**, *IDO1* **(G)** in transcriptomes of pretreatment melanoma biopsies, CancerImmu expression analysis, aggregated data from n=10 queried melanoma clinical studies, adjusted p-values, Benjamini and Hochberg procedure, LR= likelihood ratio (df=1).